

1

2

Supporting Information

3

4

5 **High-performance sandwiched-porous polybenzimidazole membrane with** 6 **enhanced alkaline retention for anion exchange membrane fuel cells**

7

8 **L. Zeng, T.S. Zhao*, L. An, G. Zhao, X.H. Yan**

9 *Department of Mechanical and Aerospace Engineering, The Hong Kong University of*

10 *Science and Technology, Clear Water Bay, Kowloon, Hong Kong SAR, China*

11 Corresponding author: Fax: (852) 23581543; Tel: (852) 23588647; E-mail: metzhao@ust.hk (T.S. Zhao)

12

1 **Experimental Section**

2 **Materials:** Graphene oxide (GO) fabricated by modified Hummers method was purchased
3 from XFNano Material Tech Co. (Nanjing, China). PBI solution (26 wt.% in N,N'-
4 dimethylacetamide (DMAc)) with intrinsic viscosity of 0.73 dl g⁻¹ was purchased from PBI
5 Performance Products Inc. All other chemicals used in the present work were of at least
6 analytical grade.

7 **Synthesis of PBI/rGO:** PBI wrapped/absorbed reduced graphene oxide (rGO) was prepared
8 by sodium borohydride reduction of GO in the presence of PBI.¹ Generally, 20 mg of GO was
9 added in a 250 mL flask, followed by the addition of 20 mL of PBI solution (4 mg mL⁻¹ in
10 DMAc). The mixture was sonicated for 60 minutes and then refluxed under magnetic stirring
11 at 140°C equipped with a water-cooling condenser for 2 hours. Thereafter, 50 mg of NaBH₄
12 was added and the mixture was refluxed for another 2 hours. The color of the mixture was
13 changed from yellow to black during the refluxing process. The suspension was centrifuged
14 with the rotating speed of 13000 rpm for 30 minutes in 5418 Centrifuge (Eppendorf). The
15 product (PBI/rGO) was collected and rinsed with copious amounts of DMAc twice. The
16 rinsed PBI/rGO was then centrifuged again and dried in a vacuum oven at 120°C overnight.

17 **Synthesis of Pd Ultrathin Nanowires (Pd NWs):** The preparation process of Pd NWs was
18 reported elsewhere.² Ethylene glycol (EG, 6 mL) solution containing poly (vinyl pyrrolidone)
19 (PVP, MW ≈55,000, 90 mg) was added into a three-neck flask equipped with a water-cooling
20 condenser and heated in an oil bath at 140°C under magnetic stirring. Then, another EG
21 solution (3 mL) containing Pd(CF₃COO)₂ (30 mg) was quickly injected with a pipette. The
22 flask was removed from the oil bath 3 hours later and naturally cooled down to room
23 temperature. The nitrogen gas (high-purity) was blanketed in the flask during the synthesis
24 process to avoid the reduction of Pd precursor by ambient air. After centrifugation and
25 washing with acetone and DI water respectively, the Pd NWs was dispersed in DI water (5
26 mL).

1 **Preparation of Pd NWs/PBI/rGO:** 10 mg PBI/rGO composite was well-dispersed in 100 mL
2 DI water under sonication. A predetermined weight of Pd NWs were slowly added and
3 deposited on PBI/rGO by stirring for 12 hours. The product (Pd NWs/PBI/rGO) was then
4 collected by centrifugation and the exact metal loading was measured by thermogravimetric
5 analysis (TGA) and inductively coupled plasma mass spectrometry (ICP-MS).

6 **Synthesis of sandwiched-porous PBI membrane (sp-PBI):** The sp-PBI membranes were
7 prepared by a pore-forming method. Generally, 2 wt.% PBI solution was mixed with dibutyl
8 phthalate (DBP) with different weight ratio under vigorous stirring. After a homogenous
9 solution was formed, the mixture was cast onto a clean glass plate using a micrometer
10 adjustable film applicator. Thereafter, the plate was introduced inside an electric oven with
11 convection air flow. To totally evaporate the solvents, the oven temperature lasted at 90°C for
12 4 hours, 120°C for 4 hours, 160°C for 6 hours and 190°C for 2 hours. Thereafter, the oven
13 temperature was steadily cooled down. The obtained PBI membranes were peeled off from
14 the glass plate. The remained DBP was totally removed by immersing PBI membranes in
15 methanol solution and the porous PBI membrane (p-PBI) was dried at 80°C in a vacuum oven
16 overnight. After that, a diluted PBI solution (1 wt.%) was sprayed on the surface of porous
17 PBI membrane on a hot electric plate. The solvents were totally evaporated at 160°C in a
18 vacuum oven. Two series of sp-PBI membranes with porosity of 40% and 60% were prepared
19 and denoted as sp-PBI40 and sp-PBI60, respectively.

20 **Material structure characterization:** Transmission electron microscopy (TEM) images
21 were obtained by operating a high-resolution JEOL 2010F TEM system with a LaB₆ filament
22 at 200 kV. The samples were dispersed in ethanol under sonication and dripped onto the holey
23 carbon-coated Cu grids. The X-ray diffraction (XRD) patterns of the samples were analyzed
24 with a Philips high resolution x-ray diffraction system (model PW 1825) using a Cu K α
25 source operating at 40 keV with the scan rate of 0.025° s⁻¹. The X-ray photoelectron
26 spectroscopy (XPS) characterization was determined by a Physical Electronics PHI 5600

1 multi-technique system using Al monochromatic X-ray at a power of 350 W.
2 Thermogravimetric analyses (TGA) was measured using a Perkin-Elmer system (TGA Q500).
3 The data were collected by heating the samples from RT to 900°C, under air atmosphere with
4 a heating rate of 10°C min⁻¹. Fourier Transform infrared spectroscopy (FTIR) measurements
5 were performed on FTS 6000 (Bio-Rad); the samples were mixed with potassium bromide
6 (KBr) and pressed into a pellet. Raman measurement was performed with a RM3000
7 (Renishaw) micro-Raman spectrometer at 514.5 nm. The laser beam was focused onto the
8 sample with a 50×objective.

9 **Porosity and alkali uptake measurement:** The membrane porosity was measured with the
10 method adapted by Mecerreyes et al.³ The weight of pristine porous PBI membrane was
11 weighted in a closed vessel (m_1). The PBI membrane was then submerged in pure methanol to
12 completely extract the pore former (DBP) and dried at 80°C in a vacuum oven overnight. The
13 weight of porous PBI membrane was then weighed in a closed vessel again (m_2). The porosity
14 (ε) was determined by:

$$15 \quad \varepsilon = \frac{m_1 - m_2}{m_1} \times 100\% \quad (1)$$

16 The dense PBI, p-PBI and sp-PBI membrane were doped in 6 M KOH for 6 days to ensure
17 that the doping process was complete. Subsequently, the membrane samples were taken out
18 and quickly wiped off with tissue papers. The membrane samples were then dried at 110°C for
19 4 hours in an oven and quickly weighed in a closed vessel (m_{dry1}) to prevent possible
20 interference from CO₂ in the air. The membrane samples were then treated in DI water at 90°C
21 for 4 hours to remove the residual KOH and dried at 110°C for 4 hours in an oven and quickly
22 weighed in a closed vessel (m_{dry2}). Accordingly, the alkali uptake (AU) were determined by:

$$23 \quad AU = \frac{m_{dry1} - m_{dry2}}{m_{dry2}} \times 100\% \quad (2)$$

24 **Ionic conductivity measurement:** The ionic conductivity of membrane samples was

1 determined with a potentiostat (EG&G Princeton, model M2273) through a two electrode
2 conductivity clamp using an AC impedance method. The membranes were sandwiched by a
3 pair of Au-coated stainless steel electrodes. The electrodes were then sandwiched between
4 two PTFE plates and placed in a humidity chamber (HP-2000, DAIHAN Labtech Co. LTD)
5 with the desired temperatures. The relatively humidity was controlled with 100% to simulate
6 the practical fuel cell operation process during the conductivity measurement. A frequency
7 range from 100 kHz to 1 Hz with a wave amplitude of 10 mV was applied to the conductivity
8 clamp to obtain the AC impedance spectra. The membrane resistance (R_{Ω}) can be obtained by
9 calculating the intercept of the high frequency region. The ionic conductivity σ can be
10 obtained from:

$$11 \quad \sigma = \frac{L}{R_{\Omega} \times A} \quad (3)$$

12 where L represents the thickness of the membrane and A represents the surface area of the
13 membrane.

14 **Electrical resistance measurement:** The electrical resistances were determined with a home-
15 made module containing a pair of gold-coated stainless steel electrode sandwiched by two
16 PTFE plates. The power samples were cold pressed into pellets with the diameter of 25 mm.
17 These pellets were sandwiched by the stainless steel electrode. The electrical resistances of
18 the pellets were determined with a potentiostat (EG&G Princeton, model M2273) through an
19 AC impedance method. The spectra were recorded at the frequency range from 10 kHz to 10
20 mHz. The DC potential was set 0 V vs. the open circuit and the wave amplitude was 10 mV.

21 **Hydrogen Permeability measurement:** Hydrogen permeability through dense PBI and sp-
22 PBI was measured with a single cell hardware (Fuel Cell Technologies, Inc). The single cell
23 was installed on a Fuel Cell Testing Equipment (Arbin Corp.), which was equipped with
24 temperature controller, mass flow-rate controllers and humidifiers for the carrier gas and
25 hydrogen gas. The membranes (23 mm in length \times 23 mm in wide \times 80 μm thickness) were

1 set in the cell. The humidified hydrogen gas (high-purity) was supplied at a flow rate of 50
2 sccm on one side of the membrane, while humidified nitrogen gas (high-purity) with the same
3 flow rate was supplied on the other side of the membrane. The pressure at both sides was
4 maintained with 10 psi during the entire measurement. After the samples were equilibrated
5 with the gases for three hours, a sample gas (2 mL) taken from the carrier gas side was
6 subjected to the gas chromatography (the Agilent 6890N gas chromatography (GC) equipped
7 with the Agilent DB-WAX 7033 capillary column).

8 **Electrochemical measurements.**

9 *Cyclic Voltammetry (CV):* Cyclic voltammetry (CV) were carried out with an electrochemical
10 workstation (Autolab PGSTAT30, Netherlands) at ambient temperature in a conventional
11 three-electrode cell. A glassy carbon electrode (GCE) with an area of 0.1256 cm² was used as
12 the working electrode, while the reference and counter electrodes were an Ag/AgCl electrode
13 and a Pt foil, respectively. GCE was polished with 0.05 μm alumina suspension and
14 ultrasonically cleaned thoroughly with DI water before each experiment. The catalyst ink
15 composed of Pd NWs/PBI/rGO and a home-made QAPPO were dispersed into 2 mL of
16 ethanol and then sonicated for 30 minutes to form a uniform suspension. Then 20 μL of the
17 catalyst ink was coated on GCE and dried in the ambient air. 0.1 M KOH was saturated with
18 nitrogen by bubbling N₂ (High-purity) for 2 hours before each experiment. The catalyst-
19 coated GCE was then subjected to electrochemical treatment by potential cycling between -
20 1.00 and +0.15 V at 50 mV·s⁻¹ in 0.1 M KOH until the stable voltammogram curves were
21 obtained (about 20 cycles). The CV curves were then obtained after scanning another 20
22 cycles and the last cycle was recorded. A flow of N₂ was maintained over the electrolyte
23 during the CV experiment. All potentials were reported versus reversible hydrogen electrode
24 (RHE). The potentials versus Ag/AgCl electrode was calibrated with respect to reversible
25 hydrogen electrode (RHE) using the following equation:

$$26 \quad E(\text{RHE}) = E(\text{Ag/AgCl}) + 0.9729 \text{ V, in } 0.1 \text{ M KOH} \quad (4)$$

1 **Rotating Disk Electrode (RDE) Measurement:** Polarization curves for oxygen reduction
 2 reaction (ORR) were performed in O₂-saturated 0.1 M KOH solution using Pine Research
 3 Instruments (Model: AFMSRCE). RDE measurement was carried out in the oxygen-saturated
 4 0.1 M KOH solution with varying rotating speeds, from 400 rpm to 2000 rpm, with the scan
 5 rate of 5 mV·s⁻¹. Koutecky-Levich plots (*i*⁻¹ vs. $\omega^{-1/2}$) were analyzed at various electrode
 6 potentials. The slopes of their best linear fit lines were used to calculate the electron transfer
 7 number (*n*) and kinetic current densities on the basis of the Koutecky-Levich equation:

$$8 \quad \frac{1}{i} = \frac{1}{j_k A_{real}} + \frac{1}{j_d A_{geo}} = \frac{1}{j_k A_{real}} + \frac{1}{B\omega^{1/2}} \quad (5)$$

9 where *i* is the measured current, *j_k* and *j_d* are the kinetic current and diffusion-limiting current
 10 densities, respectively, *A_{real}* and *A_{geo}* are the ECSA and the geometrical surface area of
 11 catalyst-coated GCE, respectively. ω is the electrode rotating rate (rpm). *B* can be calculated
 12 from the slope of the K-L equation based on Levich equation according to:

$$13 \quad B = 0.2nA_{geo}F(D_{O_2})^{2/3}\nu^{-1/6}C_{O_2} \quad (6)$$

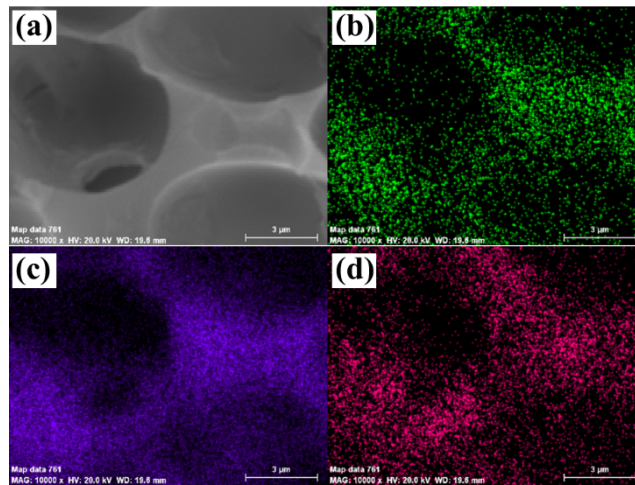
14 where *n* is the electron transfer number, *F* is the Faraday constant (*F*=96485 C mol⁻¹),
 15 *D_{O2}* is the diffusion coefficient of O₂ in 0.1 M KOH (1.86×10⁻⁵ cm² s⁻¹), ν is the kinetic
 16 viscosity (1.008×10⁻² cm² s⁻¹) and *C_{O2}* is the bulk concentration of dissolved O₂
 17 (1.21×10⁻⁶ mol cm⁻³).

18 **Membrane electrode assemblies (MEA) fabrication and fuel cell performance.** The
 19 catalyst ink composed of the Pd NWs/PBI/rGO dispersed into isopropanol was spray-coated
 20 on the both sides of the as-prepared sp-PBI membrane, making catalyst-coated membrane
 21 (CCM). The loading of the catalyst was controlled with 0.5±0.05 mg_{Pd} cm⁻² for both anode
 22 and cathode. The prepared CCM was sandwiched between two pieces of gas-diffusion layer
 23 (GDL) (SIGRACET gas-diffusion media GDL 25BC, SGL Carbon Group) to form MEAs.
 24 MEAs were then assembled in a single cell hardware (Fuel Cell Technologies, Inc) with a 5

1 cm² active area, consisting of graphite flow field plates and Au-coated steel end plates with
2 heating rods. The single cell was installed on a Fuel Cell Testing Equipment (Arbin Corp.),
3 which was equipped with mass flow-rate controllers and humidifiers for the reactant gases.
4 The contact pressure was controlled with 350 cN m⁻¹ through a torque-indicating wrench. The
5 single cell was operated at 60°C to 90°C and the H₂/O₂ humidifier temperatures were set 5 °C
6 higher than that of cell temperature. To avoid the condensation of vaporous water, the pipes in
7 both the gas inlet were also heated with the same temperature of the humidifier. Pure H₂ and
8 O₂ with the rate of 300 mL min⁻¹ and 300 mL min⁻¹ were fed into the anode and cathode
9 channel. The back pressure in the anode and cathode was maintained at 30 psi during the
10 measurement process. Humidification of the MEA was performed for 0.5 hour by flowing N₂
11 (100% RH) on both anode and cathode at a cell temperature of 60°C. MEAs were then
12 activated by cycling between OCV and 100 mV with a decrement step of 100 mV every 5
13 minutes, until stable performance between two cycles was obtained. Polarization curves were
14 collected by applying a current staircase with a duration of 5 minutes at each current. The
15 durability of MEAs was carried out at constant current.

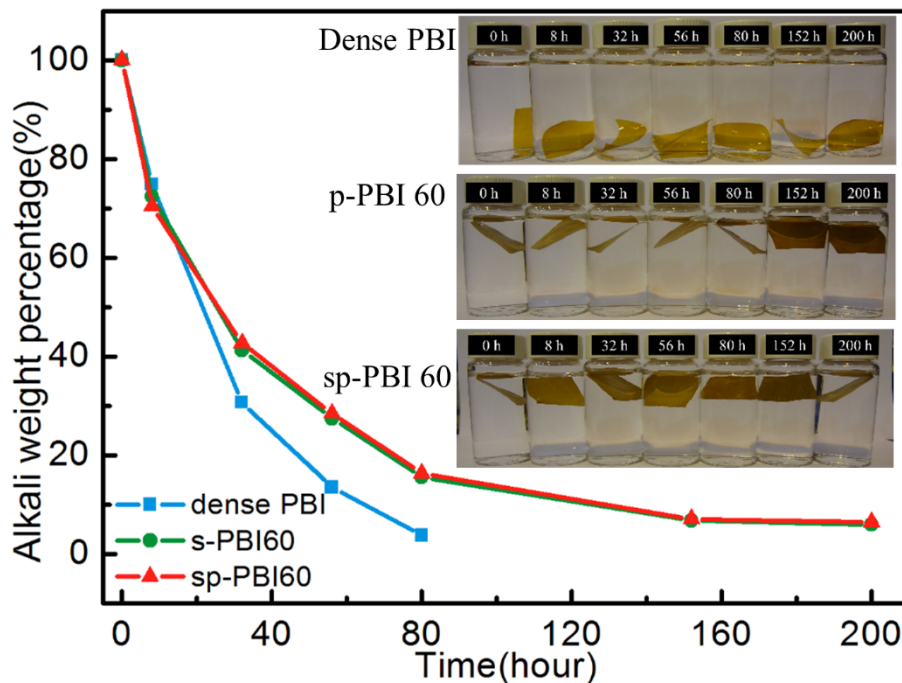
16

1
2



3
4
5
6
7
8
9

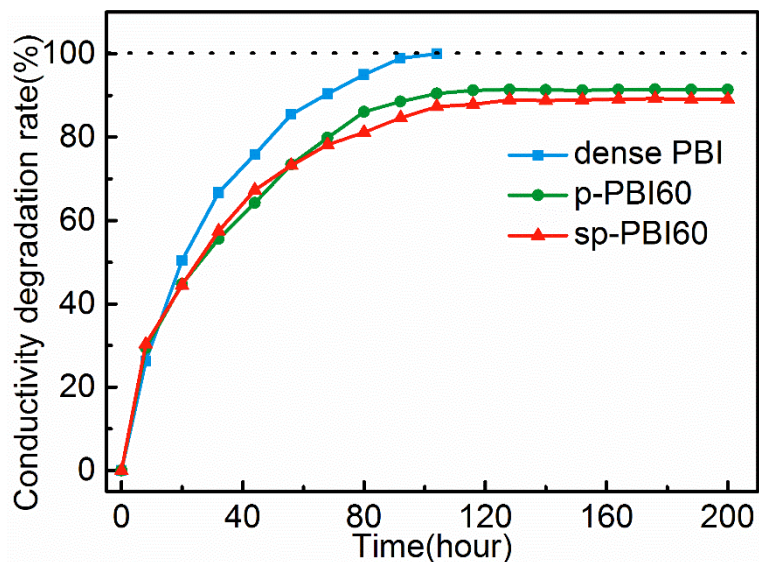
Figure S1. A typical SEM image of alkaline doped p-PBI membrane (a) and SEM-EDX mapping of nitrogen (b), potassium (c) and oxygen (d). The potassium element and oxygen element result from the doped alkaline solution. The mapping results indicate that a high level of KOH was doped on the porous walls of p-PBI.



10
11
12
13
14

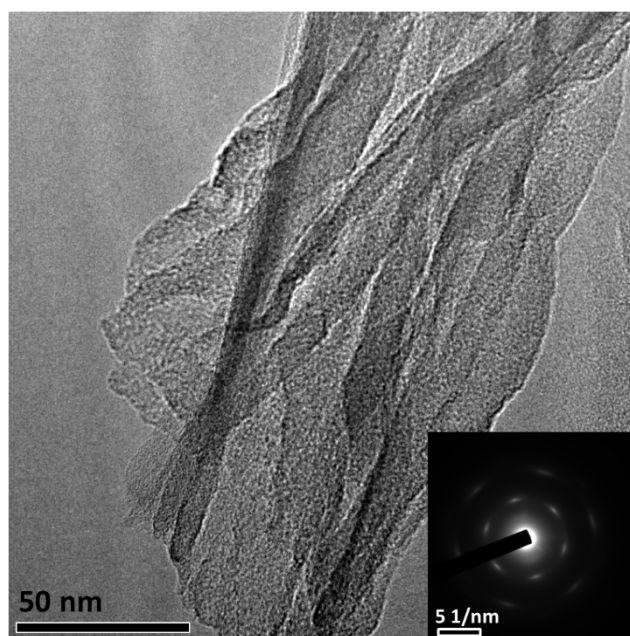
Figure S2. The curves of alkali retention percentage in the different types of PBI membranes as a function of the time. The measurement of the alkali in the PBI membranes was depicted in the supporting information.

1
2
3
4



5
6
7
8
9

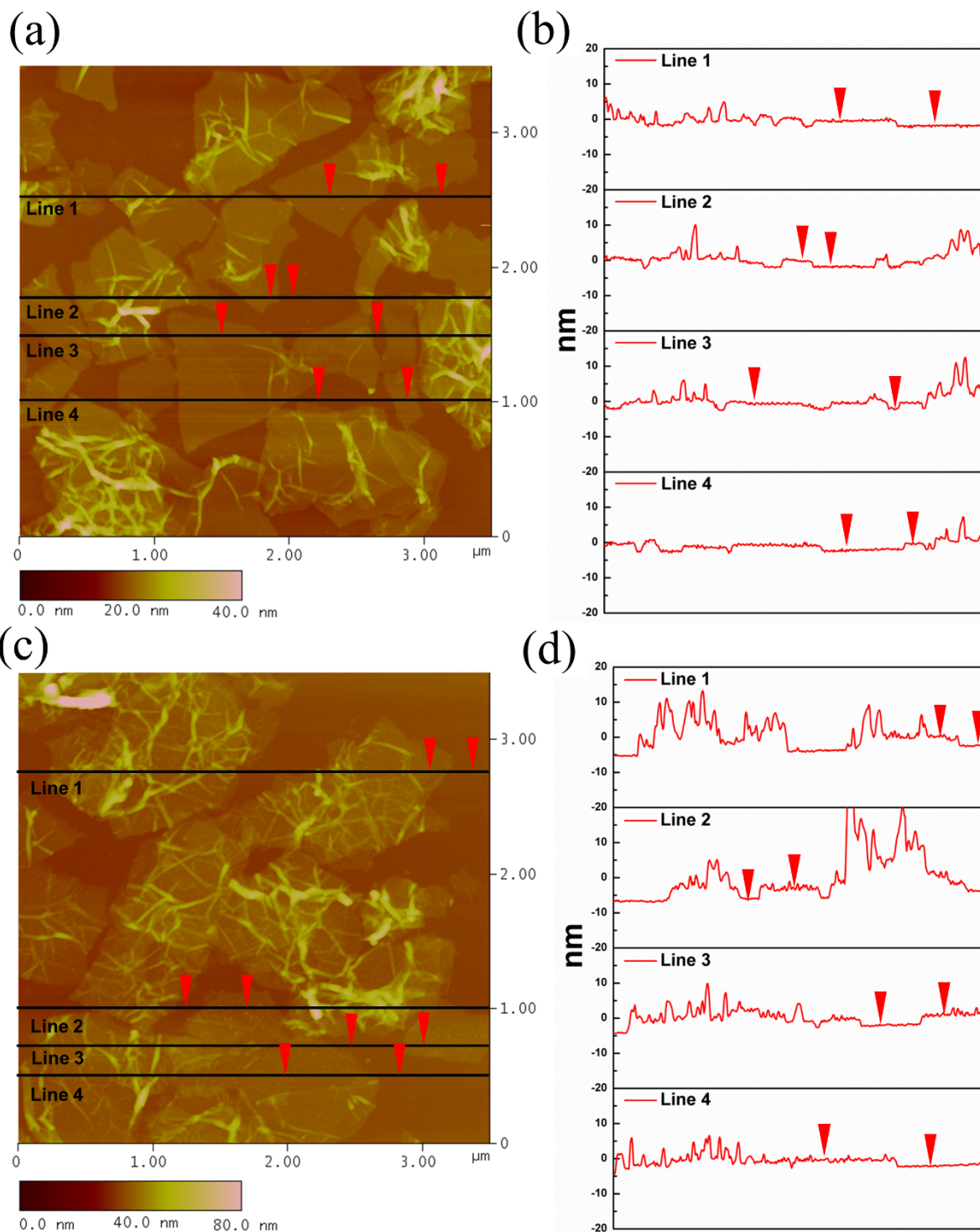
Figure S3. The curves of ionic conductivity degradation rate in the different types of PBI membranes as a function of the time.



10
11
12
13
14

Figure S4. A typical TEM image of PBI/rGO. The inset shows the diffraction pattern of a selected area electron diffraction. The well-defined diffraction spots in a hexagonal pattern demonstrated that the crystallinity of graphene was preserved during the wrapping process.

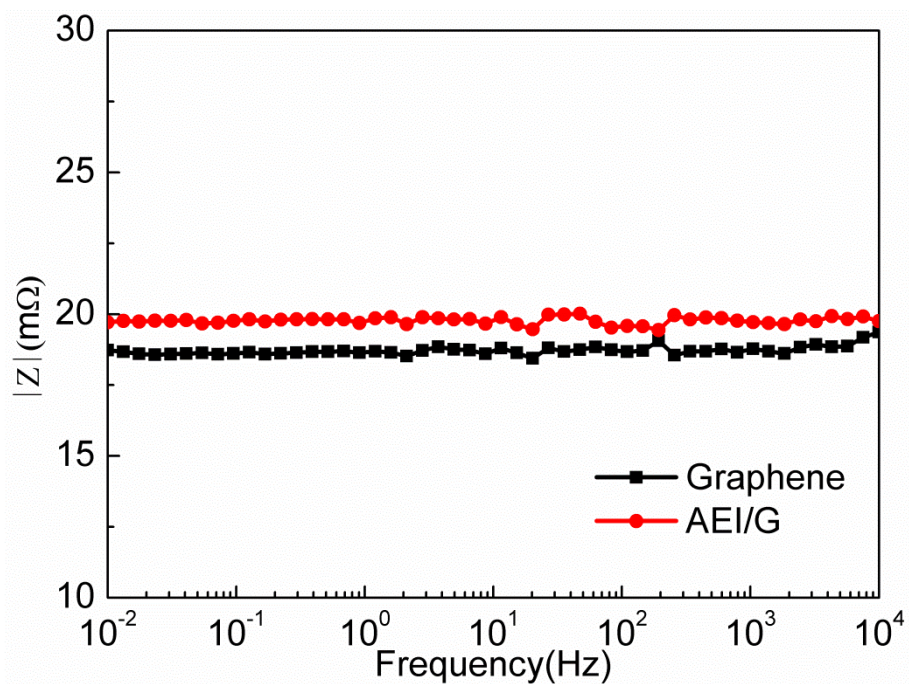
1
2
3
4



5

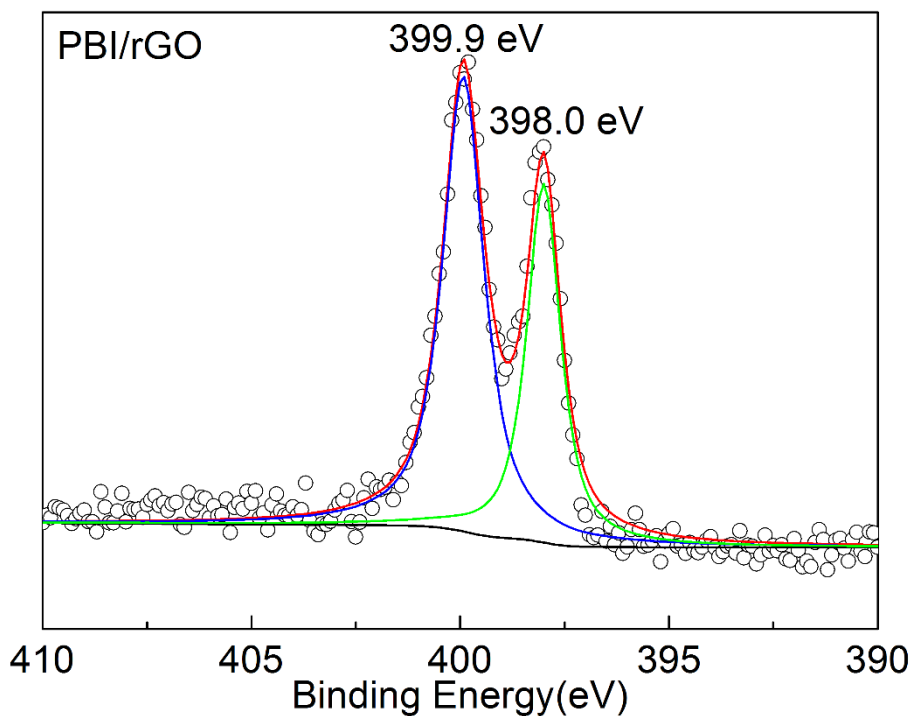
6 **Figure S5.** Tapping mode AFM images of pristine graphene nanosheets (a) and PBI/rGO (c)
7 with a large scanning area; (b) and (d) are the corresponding height profiles (red curves) along
8 the lines shown in (a) and (c), respectively.

1
2



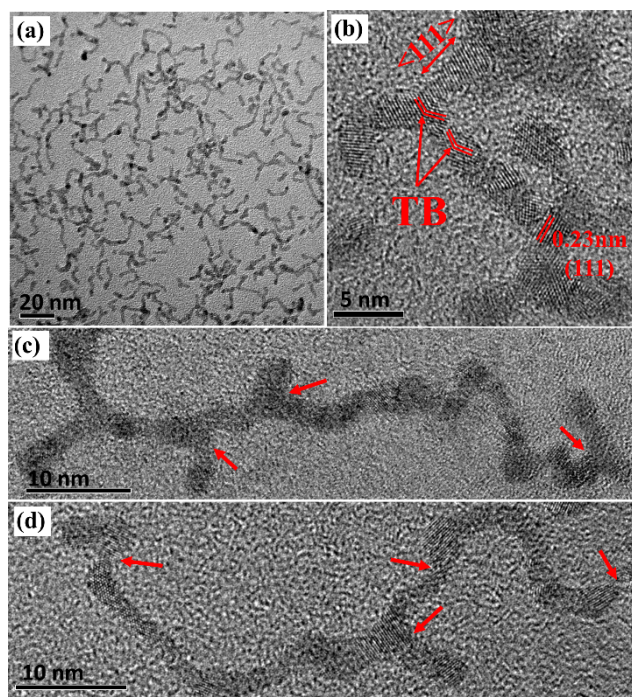
3
4
5
6

Figure S6. Bode spectra obtained through AC impedance method with an amplitude of 5.0 mV from 10 kHz to 10 mHz for graphene and PBI-wrapped graphene.



7
8
9
10

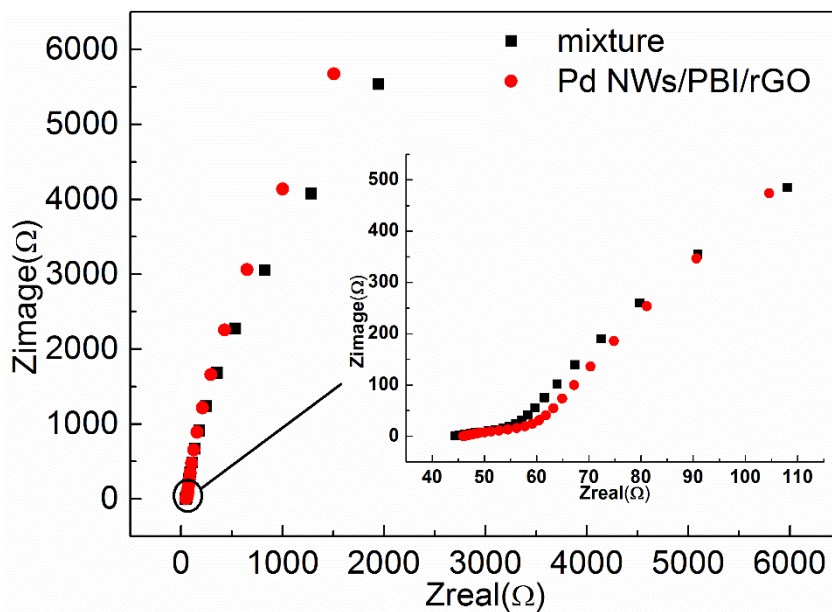
Figure S7. XPS spectrum of PBI/rGO. Symbols are experimental data and lines are deconvolution data.



1
2
3
4
5
6
7
8
9
10
11
12
13
14
15
16
17
18
19
20
21
22

Figure S8. (a) Low-resolution and (b) high-resolution TEM images of Pd NWs. The red arrows show the twin defects formed. (c) - (d) High-resolution TEM images of individual Pd NWs. The red arrows show the growth direction.

The Pd NWs were synthesized by the polyol synthesis method using $(CF_3COO)_2Pd$ as the precursor and ethylene glycol (EG) as the reductant as well as the solvent.⁴ Typical morphologies of Pd NWs are shown in Fig. S7, from which it is observed that a wavy morphology of the Pd NWs were obtained. HRTEM images (Fig. S7b) of these nanowires show clear lattice fringes with an interplanar distance of about 0.23 nm, which can be indexed to the (111) plane of the face-centered cubic-structured Pd. Interestingly, the HRTEM displayed in Fig. S7c and Fig. S7d reveals that the individual Pd NWs have diameters in the range of 2-4 nm and lengths of up to several tens of nanometers. It is also seen that each nanowire is composed of interconnected, well-crystallized Pd building blocks, which can array into nanowire morphology or merge together from different angles, as indicated by the red arrows. This mergence creates a large of twin defects, as illustrated in Fig. S7b. The formed unique wavy morphology should be ascribed to the oriented attachment mechanism. It is considered that the generated nanoparticles during the initial stage are assembled into anisotropic morphology through the merging process of the same crystal facets.^{4, 5} The peculiar wavy structure and the existence of twin defects will play an important role in the improvement of electrocatalytic activity toward oxygen reduction reaction (ORR).



1
2
3
4
5
6

Figure S9. AC impedance spectra of Pd NWs/PBI/rGO and physical mixture of Pd NWs and rGO in the three-electrode cell under otherwise identical preparation and test conditions. The magnification of high frequency section was inserted.

1
2
3
4
5
6
7
8

Table S1. Membrane porosity of different types of PBI membranes

Membrane	Predetermined porosity (%)	Measured porosity (%)
Dense PBI	0	0
p-PBI40	40	38±1.4
p-PBI60	60	57±1.9

9 The measured porosity for p-BPI membrane is slightly lower than that of predetermined
10 porosity, which is a result of the evaporation of the DBP during the membrane cast process.

11
12
13
14
15
16
17
18
19

Table S2. Permeability ($\times 10^{-17}$ mol cm cm⁻² s⁻¹ Pa⁻¹) of hydrogen for dense PBI and sp-PBI60
at different temperatures

Temperature	Pristine PBI		6 M KOH doped PBI	
	dense PBI	sp-PBI60	dense PBI	sp-PBI60
25°C	0.1	0.2	0.6	1.4
90°C	1.3	4.9	114.6	278.2

20
21
22
23
24
25
26
27
28
29
30

1
2
3
4
5
6
7
8

Table S3. Mechanical properties of pristine PBI and alkaline doped PBI membranes

Samples	Tensile strength at break(MPa)	Young's Modulus (GPa)	Elongation at break (%)
dense PBI	85.4	2.94	5.6
p-PBI60	59.6	1.79	22.2
sp-PBI60	66.6	2.09	16.8

9
10
11
12
13
14

Table S4. Half-wave potential and Pd (and Pt) specific and mass activity values

catalyst	Active surface area (m ² g ⁻¹)	half-wave potential (V)	specific activity (mA cm ⁻²)	mass activity (mA μg ⁻¹)	ref.
Pt/C		-	0.42	0.26	6
Pd/C	50 (4.9 nm)	+0.86	0.072	0.024	7
Pd/GNS	54.9 (1.80 nm)	+0.90	0.50	0.28	8
Pd/W ₁₈ O ₄₉	48.0 (19.67 nm)	+0.875	0.45	0.216	9
Pd@MnO ₂ /C	-	-	~3.75 ^a	~0.46 ^a	10
Pd-TiO ₂ /C	34 (7.1 nm)	-	0.41	-	11
hPd/C-15wt%	-	-	-	0.128	12
Pd/MWCNT	-	0.76 ^b	0.08 ^c	0.141 ^c	13
Pd icosahedra/C	- (14 nm)	-	0.50 ^a	0.055 ^a	14
Pd NWs/PBI/rGO	47.9	+0.956	0.54	0.28	This work

15 The specific and mass activity values were measured in O₂-saturated 0.1 M KOH with the rotation rate of 1600
16 rpm at room temperature unless otherwise stated.

17 a. the values were estimated from figures in this reference.

18 b. E_{1/2} was recorded with the rotation rate of 1900 rpm.

19 c. the specific area was determined at +0.85 V.

20 d. the values were determined at +1.0 V.

21
22
23

1 **Reference:**

- 2 1. M. Okamoto, T. Fujigaya and N. Nakashima, *Small*, 2009, **5**, 735-740.
3 2. Y. Wang, S. I. Choi, X. Zhao, S. F. Xie, H. C. Peng, M. F. Chi, C. Z. Huang and Y. N.
4 Xia, *Adv Funct Mater*, 2014, **24**, 131-139.
5 3. D. Mecerreyes, H. Grande, O. Miguel, E. Ochoteco, R. Marcilla and I. Cantero, *Chem*
6 *Mater*, 2004, **16**, 604-607.
7 4. Y. Wang, S. I. Choi, X. Zhao, S. Xie, H. C. Peng, M. Chi, C. Z. Huang and Y. Xia,
8 *Adv Funct Mater*, 2013.
9 5. B. Y. Xia, H. B. Wu, Y. Yan, X. W. Lou and X. Wang, *Journal of the American*
10 *Chemical Society*, 2013.
11 6. W. C. Sheng, H. A. Gasteiger and Y. Shao-Horn, *J Electrochem Soc*, 2010, **157**,
12 B1529-B1536.
13 7. L. Jiang, A. Hsu, D. Chu and R. Chen, *J Electrochem Soc*, 2009, **156**, B643-B649.
14 8. M. H. Seo, S. M. Choi, H. J. Kim and W. B. Kim, *Electrochem Commun*, 2011, **13**,
15 182-185.
16 9. Y. Lu, Y. Jiang, X. Gao, X. Wang and W. Chen, *Journal of the American Chemical*
17 *Society*, 2014.
18 10. W. Sun, A. Hsu and R. R. Chen, *J Power Sources*, 2011, **196**, 4491-4498.
19 11. S. Maheswari, P. Sridhar and S. Pitchumani, *Electrochem Commun*, 2013, **26**, 97-100.
20 12. Y. B. Cho, J. E. Kim, J. H. Shim, C. Lee and Y. Lee, *Phys Chem Chem Phys*, 2013, **15**,
21 11461-11467.
22 13. K. Jukk, N. Alexeyeva, C. Johans, K. Kontturi and K. Tammeveski, *J Electroanal*
23 *Chem*, 2012, **666**, 67-75.
24 14. G. T. Fu, X. Jiang, L. Tao, Y. Chen, J. Lin, Y. M. Zhou, Y. W. Tang and T. H. Lu,
25 *Langmuir*, 2013, **29**, 4413-4420.
26
27